Journal of Modern Optics

ISSN: 0950-0340 (Print) 1362-3044 (Online) Journal homepage: https://www.tandfonline.com/loi/tmop20

Stochastic resonance with multiplicative noise in a three-level atomic bistable system

Haibin Wu, Amitabh Joshi & Min Xiao

To cite this article: Haibin Wu, Amitabh Joshi & Min Xiao (2007) Stochastic resonance with multiplicative noise in a three-level atomic bistable system, Journal of Modern Optics, 54:16-17, 2441-2450, DOI: 10.1080/09500340701656296

To link to this article: https://doi.org/10.1080/09500340701656296

Journal of Modern Optics
Vol. 54, Nos. 16–17, 10–20 November 2007, 2441–2450

Taylor & Francis
Taylor & Francis Group

Stochastic resonance with multiplicative noise in a three-level atomic bistable system

HAIBIN WU, AMITABH JOSHI and MIN XIAO*
Department of Physics, University of Arkansas,
Fayetteville, Arkansas 72701, USA

(*Received 22 February 2007; in final form 29 August 2007*)

We experimentally investigate stochastic resonance phenomenon with multiplicative noise in a Λ-type three-level atomic bistable system. The system perturbed by a periodic low frequency forcing term shows an improved signal-to-noise ratio at certain strength of the multiplicative noise applied onto the cavity frequency.

Stochastic resonance (SR) [1–3] has been the subject of intensive research interest in past decades. It has been explored in a wide variety of physical systems, such as bistable ring lasers [4], nanomechanical systems [5], electronic and magnetic systems [6], and biological and neuronal systems [7–10]. With an external periodic perturbation applied to such two-state nonlinear systems, an addition of noise to the input of the system can induce synchronized jumps between the two stable states, showing a resonance-like peak behaviour in the signal-to-noise ratio (SNR) for certain noise strength when the noise level is scanned. Under certain conditions increasing the disorder of the input noise in a two-state nonlinear system can actually lead to an increase in the order of the output (i.e. improved SNR). It is well established that for three-level atoms, the Kerr nonlinear refractive index can be greatly enhanced due to the induced atomic coherence accompanying with reduced linear absorption [11], which can substantially modify the thresholds of the atomic optical bistability (AOB) and switching time between the bistable steady states, and control the width and height of the double-well potential (the shape of the bistable curves) [12]. These features, together with the high stability and reproducibility in the experimental setup, make the system an ideal candidate to study the detail characteristics of the SR. Studying SR in such multi-level atomic systems can help our understanding of the noise properties in these systems, and hopefully lead to new techniques to improve small signal detection and information processing in such coherent atomic systems. We have experimentally demonstrated the SR

*Corresponding author. Email: mxiao@uark.edu

Journal of Modern Optics
ISSN 0950–0340 print/ISSN 1362–3044 online
http://www.tandf.co.uk/journals
DOI: 10.1080/09500340701656296

phenomenon in a three-level AOB system, in which both the modulation signal and noise were added to the cavity input field. This is the case of additive noise, which has been well described by the generic model in the literature [2, 3]. Clear SR phenomenon was observed when the added noise strength reaches a certain optimal value for a given modulation signal strength [13]. Here, we first give some descriptions of the previous work with additive noise, and then show that the SR phenomenon can also be observed in the case with multiplicative noise, in which random noise is applied onto the cavity detuning with a modulated signal on the cavity input light. Previously such a situation has been studied less and can show some interesting features.

The generic models describing SR in an over-damped two-state system for additive and multiplicative noises are represented by the following Langevin equations, respectively [2, 3, 14]:

$$\dot{x} = -\mathrm{V}'(x) + A_0 \cos \omega t + \xi_A(t) \tag{1}$$

and

$$\dot{x} = -\mathrm{V}'(x) + x\xi_M(t) + A_0 \cos \omega t \tag{2}$$

with

$$V(x) = -\frac{a}{2}x^2 + \frac{b}{4}x^4,$$

where A_0 is the signal amplitude and ω is the frequency of the signal. x is the quantity of interest for a given system, for example, the position of a harmonic oscillator. In our model, x represents the cavity field amplitude. ξ_A, ξ_M are zero-mean valued, Gaussian white noises with autocorrelations $\langle \xi_i(t)\xi_j(0)\rangle = 2D_i\delta_{ij}(t)$, where D_i characterizes the noise strength for either the additive or the multiplicative noise case. The potential $V(x)$ represents a double-well potential under certain parametric conditions (when parameters a and b have the same sign). In our system of three-level atoms inside an optical cavity, the parameters a and b are determined by many experimental parameters such as frequency detunings and the coupling laser power.

Equation (1) represents a response of additive noise with an additive modulation. Equation (2) is for a system with a periodic modulation and applied multiplicative noise. In equation (1), at $A_0 = 0$, the stationary probability distribution of finding the state at x is given in general by [15, 16]

$$P(x) = N_0 \exp\left(-\frac{V(x)}{D_A}\right),$$

where N_0 is a normalization constant. In the presence of a small periodic modulation and under low frequency approximation, the depth of each potential well changes alternatively on the half period. The effective potential can be expressed as

$$V(x, t) = V(x) - A_0 x \cos \omega t.$$

In equation (2), under the adiabatic approximation, the probability of finding the state at x can be written as [14]

$$P(x,t) = N_M x \exp\left(-kx^2 - \frac{A_0 \cos \omega t}{D_M |x|}\right),$$

where N_M is a normalization constant and $k = a/2D_M$. Such simple, generic models (equations (1) and (2)) have been used to study the noise properties of bistable systems [14]. In the current system, x is the intracavity field (also the probe field for the three-level atoms).

Our experimental setup is shown in figure 1. A three-level Λ-type atomic medium is placed inside an optical ring cavity. The energy levels of the D_1 line of the ^{87}Rb atom are employed to form the three-level system as shown in the inset of figure 1. A coupling laser (LD2) of frequency ω_c near the ω_{23} resonance couples level $|3\rangle$ and

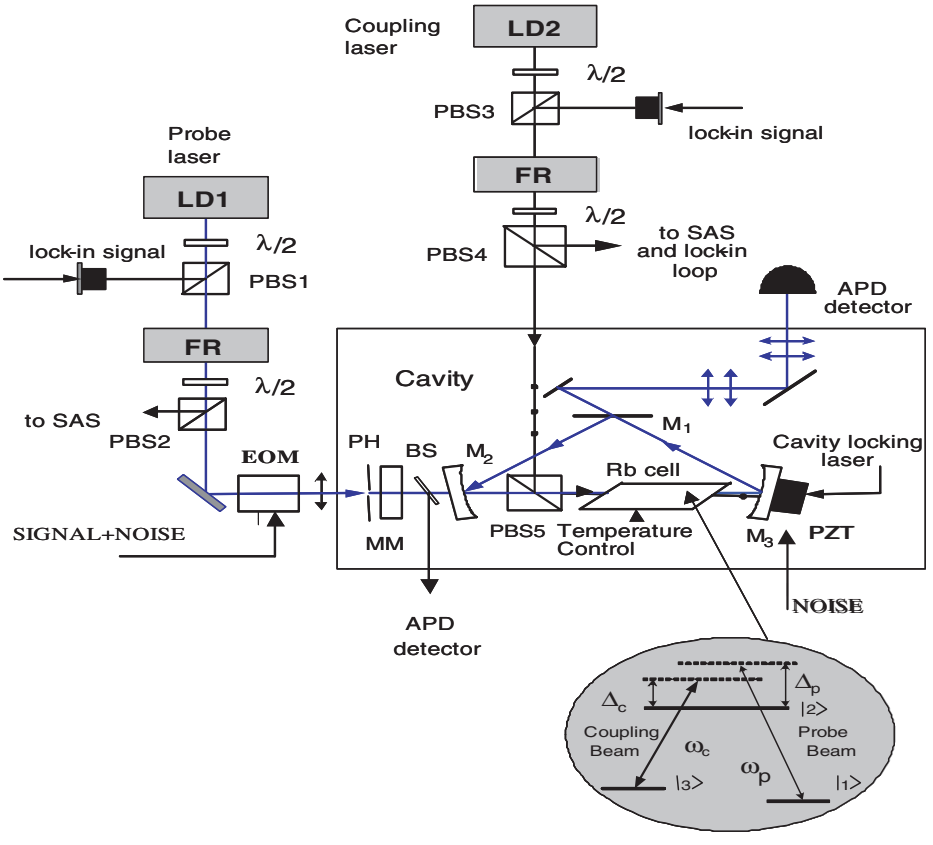

Figure 1. Experimental setup. LD1 and LD2, diode lasers; EOM, electro-optic modulator; PBS, polarizing cubic beam splitters; M1–M3, cavity mirrors; APD, avalanche photodiode detectors; PZT, piezoelectric transducer; MM, mode matching lens; PH, pin hole. The bubble shows a three-level system in Λ configuration. (The colour version of this figure is included in the online version of the journal.)

level $|2\rangle$, while a probe laser beam (LD1) with frequency ω_p near the ω_{21} resonance drives the transition from level $|1\rangle$ to level $|2\rangle$. Δ_c and Δ_p are their respective frequency detunings defined by $\Delta_c = \omega_c - \omega_{23}$ and $\Delta_p = \omega_p - \omega_{21}$, respectively. The optical ring cavity has three mirrors, two of which have about 1% (M1) and 3% (M2) transmissivities, respectively, while the third one (M3) is assumed to be an ideal reflector and is mounted on a piezoelectric transducer (PZT) for scanning cavity length. The cavity frequency detuning is defined by $\Delta_\theta = \omega_{cav} - \omega_{21}$, where ω_{cav} is the cavity resonance frequency. The rubidium vapour cell is wrapped in metal foil for protection from external magnetic field disturbance and then heat tape for atomic density control is added outside the foil. The probe laser beam circulates inside the cavity as the cavity field, while the coupling beam is injected into the cavity through a polarization beam splitter (PBS5) that is misaligned slightly from the probe beam (about 2° angle) so it will not circulate in the cavity. Both the probe and coupling lasers are extended cavity diode lasers and are frequency stabilized. The frequency detunings of the lasers from their respective atomic transitions are set and monitored separately by using a saturated atomic spectroscopy setup (not shown in figure 1). One of the advantages of our experimental system is the use of the two-photon Doppler-free configuration [12]. By propagating the coupling and probe (cavity) laser beams collinearly through the atomic vapour cell containing three-level Λ-type rubidium atoms, the first-order Doppler effect is eliminated even in an atomic vapour cell, which greatly reduces the experimental complications.

The first step in the experiment was to lock the frequencies of both the coupling and probe lasers. The coupling laser was tuned and locked to the $5S_{1/2}$, $F = 2$–$5P_{1/2}$, $F' = 2$ transition, while the probe laser was tuned and locked to the $5S_{1/2}$, $F = 1$–$5P_{1/2}$, $F' = 2$ transition in ^{87}Rb. Next, we locked the optical ring cavity with the help of a third diode laser. Then the electro-optic modulator (EOM) in the path of the cavity input beam is switched on with a saw-tooth voltage to scan the intensity of the cavity input beam. By adjusting the appropriate experimental parameters (Δ_c, Δ_p, Ω_c, Δ_θ) [12] one can easily get the bistable curve in the input–output intensity plot as shown in figure 2. After the bistable curve is obtained, all experimental parameters are fixed and the saw-tooth voltage on the EOM is then switched off. The intensity of the cavity input beam was adjusted, so it stays in the low state within the bistable region. Then we superimpose a sinusoidal signal and a Gaussian noise onto the cavity input beam through the EOM. The time series of the input and output beams are detected by APD detectors and stored digitally in the oscilloscope and then a fast Fourier transform (FFT) is performed to get the power spectrum. The SNR used here is defined as the ratio between the magnitude of the power spectrum at the signal frequency with the input signal and without the signal turned on [2]. Figure 3 is the SNR of the cavity output field as a function of the noise strength normalized by the width of the bistable curve. The experimental parameters are: $T = 68°\text{C}$, $P_c = 12\,\text{mW}$, $\Delta_c = 150\,\text{MHz}$, $\Delta_p = 100\,\text{MHz}$ and cavity detuning $\Delta_\theta = 50\,\text{MHz}$. From the figure one can clearly see that the SNR has a resonance-like peak at a certain medial noise level and the result of the experimentally measured curve matches well with the theoretical prediction given by the generic model of equation (1) with similar parameters. These results indicate that the SR observed in our three-level AOB system with additive noise can be well

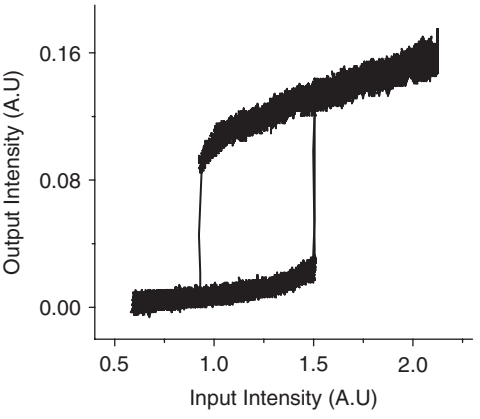

Figure 2. A typical bistable curve. The experimental parameters are: $T = 69^{\circ}\mathrm{C}$, $\Delta_c = 96\,\mathrm{MHz}$, $\Delta_p = 160\,\mathrm{MHz}$, $P_p = 14\,\mathrm{mW}$, $P_c = 27\,\mathrm{mW}$ and $\Delta_\theta = 50\,\mathrm{MHz}$.

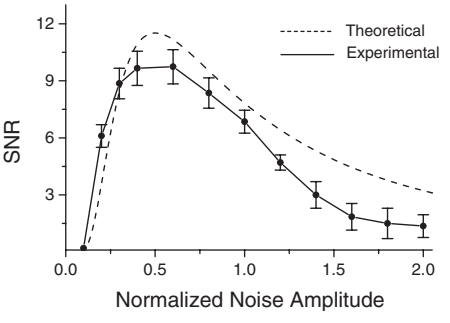

Figure 3. Output SNR as a function of input noise amplitude. The x axis represents twice the standard deviation of the noise amplitude divided by the width of the bistable region. Figure is from [13] with modification. Reprinted figure with permission from A. Joshi and M. Xiao, Phys. Rev. A **74** 013817 (2006). Copyright (2006) by the American Physical Society.

described by the simple generic model of the double-well potential [2, 3]. Such a case of additive noise in the three-level bistable system has been studied in detail previously [13].

Next, we only apply the modulation signal onto the cavity input field through the EOM, and applied random noise onto the cavity detuning through the PZT mounted on one of the cavity mirrors (M3). We investigate changes of the SNR of the cavity output field as a function of the applied noise strength under this configuration. For a refractive AOB hysteresis curve, the parameters a and b in equation (2) are mainly related to the cavity detuning and the third-order nonlinear susceptibility of the medium, respectively [17], so the system evolution can be approximately described by equation (2) as the case of multiplicative noise. Of course, other parameters, such as coupling beam frequency detuning and amplitude, as well as probe detuning, will also contribute to the shape of the potential. The exact

dependences of a and b in equation (2) on experimental parameters (Δ_c, Δ_p, Ω_c, Δ_θ) are very complicated and hard to be given in such a simple form. After the hysteresis curve is obtained, a small mount of random noise is applied onto the cavity frequency through the PZT. To see the influence of the change of cavity frequency detuning due to the applied noise, we first look at the steady-state bistable curves at different noise strengths. Several stationary bistability curves are presented in figure 4 at different noise levels. We can clearly see that although the thresholds of AOB curves fluctuate under the applied noise, the bistable curves are not fundamentally changed at the noise levels used in the experimental measurements. The adiabatic approximation still holds well in such circumstances with the low frequency scan of the input field intensity [18]. For a given noise strength, the bistable curve has two threshold values going up and two going down, as shown in the curves of figure 4. Even for quite large noise strengths, clear bistable hysteresis loops are clearly preserved.

Now, we stop scanning the cavity input intensity and set it at the middle of the bistable curve at its lower branch. By applying the noise on the cavity frequency detuning (which is modelled as multiplicative noise, as described by equation (2)), the cavity field can jump from the lower branch to the upper branch. When the

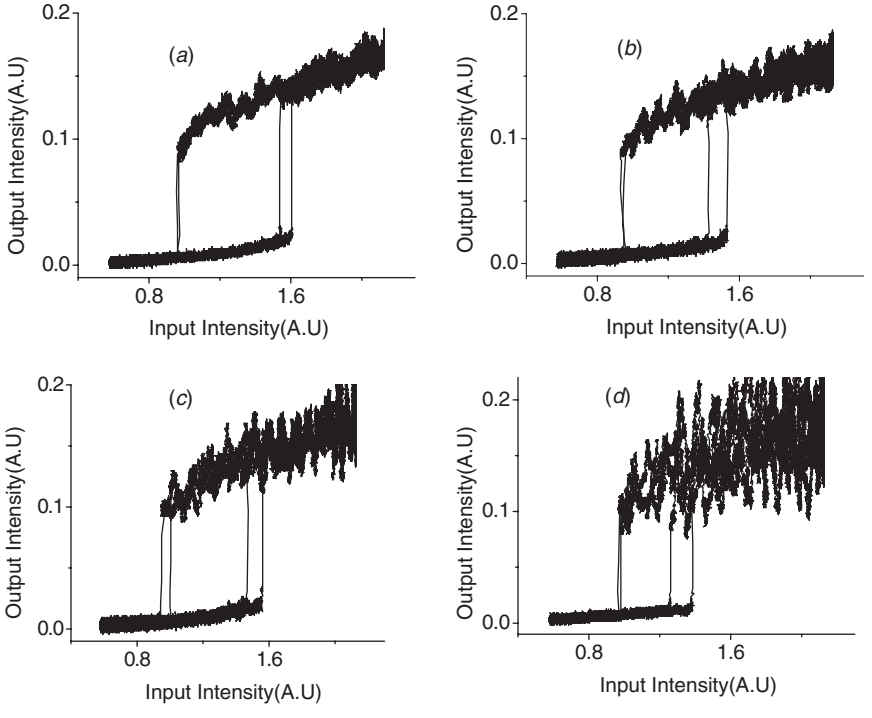

Figure 4. The bistable curves with different noise amplitudes: (*a*) $\kappa = 5\,\text{mV}$, (*b*) $\kappa = 21.5\,\text{mV}$, (*c*) $\kappa = 40.1\,\text{mV}$, (d) $\kappa = 56.3\,\text{mV}$. κ is the standard deviation of noise amplitude. Other parameters are: $T = 69^\circ\text{C}$, $\Delta_c = 96\,\text{MHz}$, $\Delta_p = 160\,\text{MHz}$, $P_p = 14\,\text{mW}$ and $P_c = 27\,\text{mW}$.

noise level is low ($\kappa = 5$ mV, where κ is the standard deviation of noise amplitude), the probability of jumping events is quite low as shown in figure 5(*a*). At such noise strength, the bistable curve is very stable (as shown in figure 4(*a*)), so such a jump is rare between the two bistable states through the potential barrier. As the noise strength is increased, the probability of jumping events can be greatly increased, as shown in figures 5(*b*)–(*d*). At intermediate noise levels (figures 5(*b*) and (*c*)) the jumping events are more regulated and time intervals between jumping events are almost similar, and are correlated with the signal frequency in figure 5(*b*) in which there is almost a transition from the low state to the upper state in every half period of the input signal. As the noise strength is further increased, many transitions are activated and the synchronization between the signal and noise is lost, and jumping events become random again, since the signal is now buried under the large noise, as shown in figure 5(*d*). Furthermore, one can clearly see in figure 5(*d*) that the intrawell motion becomes more evident, which is not our main interest here. Even for quite large noise strength, the bistable curves are still quite stable as shown in figures 4(*b*)–(*d*). Then a FFT of the time series is performed to get the

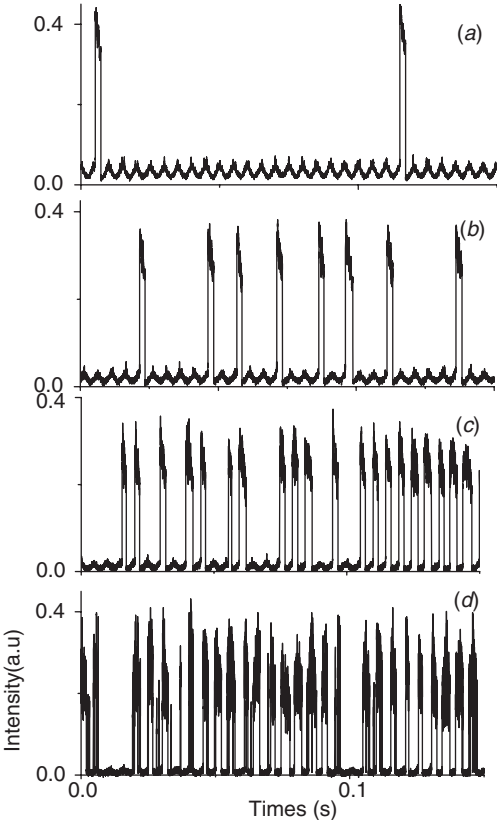

Figure 5. Time series of the cavity output field for various noise strengths (increasing from top to bottom: $\kappa = 5$, 10.2, 21.7 and 49.1 mV) and for a modulation frequency of 200 Hz.

power spectrum. A typical power spectrum of the cavity output field measured in the experiment is shown in figure 6. This power spectrum shows a clear peak at the modulation frequency and a weaker peak at its harmonic on a Lorentzian noise background. The appearance of the second harmonic peak here is probably caused by a small residual asymmetry in the unmodulated potential [19]. When the SNR is plotted as a function of noise strength, as shown in figure 7, a resonance-like maximum appears at intermediate noise strength. This SNR plot is normalized to the maximal value to just show the SR effect. Some small peaks also appear at both sides of the major peak, we do not have a simple explanation for them at this time. It seems that the accurate model for the system is more complicated than the one

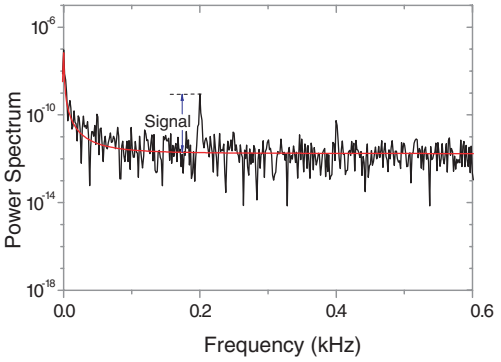

Figure 6. A typical power spectrum (at signal frequency 200 Hz, $\kappa = 14.8$ mV, normalized) for the output of the optical cavity. (The colour version of this figure is included in the online version of the journal.)

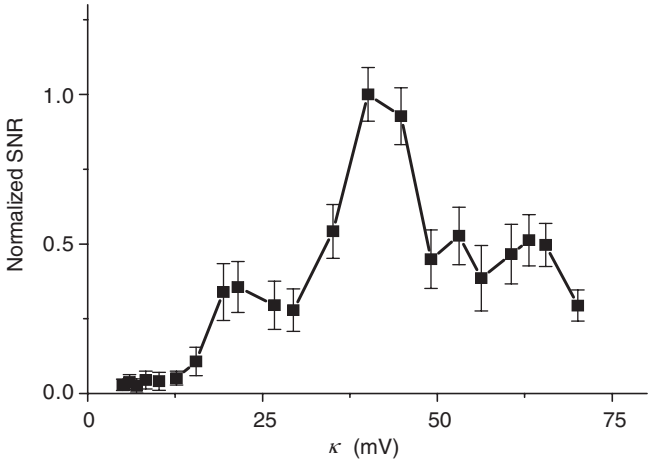

Figure 7. SNR (normalized) of cavity output field measured as a function of cavity noise amplitudes. Modulation frequency and amplitude are 200 Hz and 70 mV, respectively. Other parameters are same as in figure 4.

described by equation (2) and is difficult to obtain. First, our current system is more complex and a multi-dimensional system, and even with appropriate adiabatic eliminations one Langevin equation, such as equation (2), is not enough to describe the system dynamics. Second, the detail of exactly how the bistable potential is modulated in the three-level AOB system is not well understood and can contribute to the SR behaviour. The effect of multiple thresholds due to applied noise on the cavity frequency detuning (multiplicative noise), as shown in figure 5, is more complicated than the case of additive noise on the cavity input field studied previously. The experimental parameters used in the experiment are: $T = 69^{\circ}\mathrm{C}$, $\Delta_c = 96\,\mathrm{MHz}$, $\Delta_p = 160\,\mathrm{MHz}$, $P_p = 14\,\mathrm{mW}$, $P_c = 27\,\mathrm{mW}$ and modulation frequency 200 Hz.

Since the noise is applied on the cavity frequency detuning, we need to consider it as multiplicative noise, such as the one described by equation (2), which is different from the additive noise as described by equation (1). The treatment of multiplicative noise is much more complicated and significant differences can exist compared to the additive noise cases, which have been more well studied and understood. More theoretical modelling is needed to fully understand the current system.

In summary, we have experimentally researched the SR phenomenon in a three-level AOB system with additive noise (noise added on cavity input beam) and multiplicative noise (noise applied onto the cavity frequency detuning), respectively. Clear improvements in SNR were observed in both cases at certain noise strengths. The case of multiplicative noise turns out to be much more complicated and more theoretical modelling is needed to fully understand such behaviour. The experiments demonstrated different ways to improve SNR in a system by applying a certain amount of noise. Noise-induced bistable steady states have been observed and can be controlled by applying modest noise on the cavity frequency detuning, which can be used to make controllable optical switches.

Acknowledgements

Funding support from the National Science Foundation is acknowledged.

References

[1] R. Benzi, A. Sutera and A. Vulpiani, J. Phys. A **14** 453 (1981).
[2] L. Gammaitoni, P. Hanggi, P. Jung, *et al.*, Rev. Mod. Phys. **70** 223 (1998), and references therein.
[3] T. Wellens, V. Shatokhin and A. Buchleitner, Rep. Prog. Phys. **67** 45 (2004), and references therein.
[4] B. McNamara, K. Wiesenfeld and R. Roy, Phys. Rev. Lett. **60** 2626 (1988).
[5] R.L. Badzey and P. Mohanty, Nature **437** 995 (2005).
[6] S. Fauve and F. Heslot, Phys. Lett. **97** 5 (1983).
[7] P. Jung and K. Wiesenfeld, Nature (London) **385** 291 (1997).
[8] J. Grohs, S. Apanasevich, P. Jung, Phys. Rev. A **49** 2199 (1994).
[9] F. Moss and K. Wiesenfeld, Sci. Am. **273** 50 (1995)
[10] K. Wiesenfeld and F. Moss, Nature (London) **373** 33 (1995)

[11] H.Wang, D. Goorskey and M. Xiao, Phys. Rev. Lett. **87** 073601 (2001)
[12] A. Joshi, A. Brown, H. Wang, *et al.*, Phys. Rev. A **67** 041801(R) (2003); A. Joshi and M. Xiao, Phys. Rev. Lett. **91** 143904 (2003); A. Joshi, W. Yang and M. Xiao, Phys. Rev. A **70** 041802(R) (2004).
[13] A. Joshi and M. Xiao, Phys. Rev. A **74** 013817 (2006).
[14] L. Gammaitoni, F. Marchesoni, E. Menichella-Saetta, *et al.*, Phys. Rev. E, **49** 4878 (1994).
[15] P. Hanggi, P. Talkner and M. Borkovec, Rev. Mod. Phys. **62** 251 (1990).
[16] N.G. Vankampen, *Stochastic Process in Physics and Chemistry* (Elsevier, Amsterdam, 1997).
[17] H. Risken, C. Savage, F. Haake, *et al.*, Phys. Rev. A **35** 1729 (1987).
[18] A. Joshi, W. Yang and M. Xiao, Opt. Lett. **30** 905 (2005).
[19] T. Zhou and F. Moss, Phys. Rev. A **41** 4255 (1990).